Kinetico-Mechanistic Studies of Cu(II)-Mediated Cyclization of Imines via C–H Bond Activations

Daniel Pla, Montserrat Ferrer, Montserrat Gómez, Manuel Martinez Lopez

EurJIC
European Journal of Inorganic Chemistry

Research Article
doi.org/10.1002/ejic.202400564

Chemistry Europe
European Chemical Societies Publishing

www.eurjic.org

Kinetico-Mechanistic Studies of Cu(II)-Mediated Cyclization of Imines via C–H Bond Activations

Daniel Pla,[a] Montserrat Ferrer,[b, c] Montserrat Gómez,*[a] and Manuel Martinez Lopez*[b, c]

Dedicated to Rudi van Eldik for his 80th birthday.

Herein, we focus on the kinetico-mechanistic studies of a carboxylate and Cu(II)-assisted synthesis of imidazo[1,5-*a*]pyridines encompassing C(sp^3)–H amination and cyclization of imines coupled with C(sp^2)–H cyanation using time-resolved UV-Vis reaction monitoring and *ex-situ* analyses. Thus, kinetic studies have been carried out, providing a proof of the elementary steps involved, allowing for batch analysis of the compounds present in solution *via* MS. The experimental data obtained are consistent with the formation of a cyclometalated complex (k_1) involving a C(sp^3)–H bond cleavage followed by a reductive elimination/proton abstraction event (k_2), both showing high enthalpy-demanding transition states. The two processes show a well-defined Eyring behavior with values of $\Delta H^{\neq}$ and $\Delta S^{\neq}$ within the expected range. Further insights on the intermediate fast C(sp^2)–cyanation are also presented together with control reactions.

1. Introduction

C–H Bond activation represents a highly attractive topic in catalysis leading to valuable transformations. The functionalization of C–H bonds in a selective and efficient manner is especially challenging in the case of C(sp^3)–H ones, in particular using non-noble metals.[1] Among 3d transition metals, copper is an Earth-abundant element of relevance in catalysis due to its high functional group tolerance and low toxicity, two facts that are key to streamline C–H amination and cyanation processes needed for sustainable synthesis of aza-heterocycles in high atom economy and low environmental impact.[2]

The mechanistic understanding of the elementary C–H bond metalation steps enables a better insight not only in the selectivity of transition-metal-mediated organic transformations, but also in the oxidation states of metal centers involved. In addition to classical metalations (*i.e.* σ-bond metathesis with early transition metals, oxidative addition with electron-rich late transition metals or electrophilic activation with electron-deficient ones),[3] recent evidences on novel C–H bond metalation mechanisms, where the oxidation state of the metal center remains unchanged thanks to the assistance of directing groups with Lewis-basic properties,[4] have been reported as concerted metalation deprotonation (CMD)[5] or amphiphilic metal-ligand activation (AMLA).[6] Besides, electrophilic Cu(III) species have also been proposed in the frame of both C(sp^3)–H bond cyanation[7] and amidation[8] processes in the presence of oxidizing reagents (such as *N*-fluorobenzenesulfonimide, [N-(C_4H_9)$_4$]$_2$[Ce(NO_3)$_6$] and duroquinone) to facilitate reductive elimination events in Cu(III)/(I) manifolds.

Nitrogen-based heterocycles such as purines, pyrimidines, pyridines and triazines are of particular interest in medicinal chemistry because they are present in a wide variety of natural products and also in drugs.[9] Thus, Cu-based catalytic methodologies involving the activation of robust C(sp^3)–H bonds of nitrogenated starting compounds represent a sustainable way to access these privileged scaffolds. In this frame, we have recently prepared a family of imidazo-pyridines by functionalization of C(sp^3)–H bonds of imines.[10]

In the quest towards assessing the experimental relevance of organocopper species in catalysis (organocopper(II)[11] and Cu(III)[12] being highly elusive due to either the intrinsic reactivity of the Cu–C bond or plausible ligand oxidation processes),[13] herein we report the kinetico-mechanistic insights from the study of a multiple copper-mediated C–H functionalization in α and α′ positions of a pyridinylimine towards the synthesis of imidazo[1,5-*a*]pyridine heterocycles. The studies have been conducted by operando UV-Vis reaction monitoring coupled to *ex-situ* HPLC-MS analyses, in an attempt to gain a better experimental insight on the reaction mechanism and the transient organometallic species involved.[10]

[a] *D. Pla, M. Gómez*
Laboratoire Hétérochimie Fondamentale et Appliquée, UMR CNRS 5069, Université Toulouse 3 – Paul Sabatier, 118 route de Narbonne, 31062 Toulouse Cedex 9, France
E-mail: Montserrat.gomez-simon@univ-tlse3.fr

[b] *M. Ferrer, M. Martinez Lopez*
Departament de Química Inorgànica i Orgànica, Secció de Química Inorgànica, Universitat de Barcelona, Barcelona 08028, Spain
E-mail: manel.martinez@qi.ub.es

[c] *M. Ferrer, M. Martinez Lopez*
Institute of Nanoscience and Nanotechnology (IN2UB), Universitat de Barcelona, Barcelona 08028, Spain

Supporting information for this article is available on the WWW under https://doi.org/10.1002/ejic.202400564

Research Article
doi.org/10.1002/ejic.202400564

Experimental Section

The general information related to chemicals and instruments is given in the Supplementary Information.

Ex-Situ Reaction Monitoring in the Absence of 2,3-dichloro-5,6-dicyano-1,4-benzoquinone (DDQ)

A mixture containing **1 a** (64.0 mg, 0.39 mmol) and $Cu(OPiv)_2$ (103.1 mg, 0.39 mmol) in MeCN (5 mL) was stirred at 70 °C and aliquots (200 μL) taken at 3, 12, 48 and 90 h were analyzed by MS (ESI).

Ex-Situ Reaction Monitoring in the Presence of DDQ

DDQ (87.4 mg, 0.39 mmol) was added to a solution of **1 a** (64.0 mg, 0.39 mmol) and $Cu(OPiv)_2$ (103.1 mg, 0.39 mmol) in MeCN (5 mL). The reaction mixture was stirred at 70 °C and aliquots (200 μL) were taken at 2, 3, 10, 12, 24 and 48 h and analyzed by HPLC-MS (ESI) and HRMS (ESI).

Kinetics

The kinetic profiles for the reactions were followed by UV-Vis spectroscopy in the full 1100–200 nm range on an HP8453 instrument equipped with a thermostated multicell transport. Observed rate constants were derived from absorbance *versus* time traces at the wavelengths where a maximum increase and/or decrease of absorbance were observed; alternatively, the full spectral time-resolved changes where used. The calculation of the observed rate constants from the absorbance *versus* time monitoring of reactions were carried out using the SPECFIT or ReactLab softwares,[14] with an A→B→C consecutive kinetic model. Both software packages are based on the Global Analyses chemometric perspective; the time-resolved full spectral changes (time/wavelength/absorbance matrixes) in the reacting solution are considered without establishing structural characteristics for any of the components,[15] thus allowing for the detection of reaction intermediates even at low relative concentrations.[16] Table S1 collects all the derived values of these constants (errors comprised within the 15% margin). The general kinetic technique is that previously described;[3a,5c,17] all measures were conducted by adding the needed amounts of carefully degassed and nitrogen-flushed stock solutions of the different components to the calculated amount of solvent inside nitrogen-flushed UV-Vis cells. It is to note that in the present study, and given the high temperatures and the long times required for the monitoring, the 1 cm cells utilized had a screw tap with Teflon sealing covers to avoid evaporation of the solvent. In all cases, the cell was filled up to a 95% of their capacity to avoid refluxing artefacts during the measures at temperatures close to the boiling point of the solvent.

The presence of metallic copper, formed when **1 a** is reacted in a 1:1 ratio with $Cu(OPiv)_2$, was not found to interfere in the processes conducted due to the extremely low concentration of the reactants (in the order of 10^{-5} M) in the runs, that is, runs were found totally equivalent in the presence or absence of polyvinylpyrrolidone which is known to stabilize colloidal Cu^0 nanoparticles solutions.

ESR Spectroscopy

The ESR spectra were carried out by the Mesures Magnètiques unit of the Scientific and Technological Centers of the Universitat de Barcelona (CCiTUB), using a Bruker CW/FT-ESR ELEXSYS E580XQ-10/12 CW ESR spectrometer system, with the SHQE cavity, at 77 K in acetonitrile solution and a flat cell for room temperature measurements.

2. Results and Discussion

Based on our previous results on the Cu(II)-mediated synthesis of imidazo[1,5-*a*]pyridine derivatives from preformed imines (**1**),[10] we have studied the mechanism leading to the formation of two types of aza-heterocycles. One of them is formed involving the activation of two C(sp^3)–H bonds (**2**) and another involved the same C(sp^3)–H bonds *plus* an additional C(sp^2)–H bond (**3**) (Scheme 1). Compounds **2** are obtained under stoichiometric conditions with 1 equivalent of copper pivalate, while compounds **3** are typically obtained under catalytic conditions (30 mol% of Cu(II)) in the presence the 2,3-dichloro-5,6-dicyano-1,4-benzoquinone (DDQ) oxidant, which serves both as cyanating agent and oxidant towards closing the catalytic cycle.[10] It is also important to note that although the reaction is carried out in acetonitrile it also takes place when cyclopenthyl-methyl ether is used as solvent, indicating that the solvent is not the source of cyano groups in compounds **3**.[10] For the kinetic studies, the imine **1 a** was chosen.

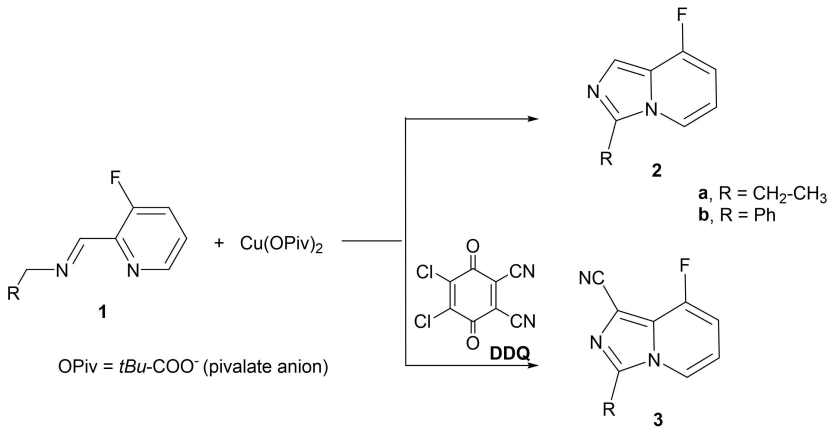

Scheme 1. Cu(II)-mediated synthesis of aza-heterocycles (**2** and **3**) from iminopyridines (**1**).

Research Article
doi.org/10.1002/ejic.202400564

2.1. Time-Resolved Monitoring of the Proposed Steps Under Stoichiometric Conditions

2.1.1. Reaction in the Absence of DDQ

For the mechanistic study on the formation of **2a** (Scheme 1) time-resolved UV-Vis spectroscopy monitoring of the stoichiometric reaction between imine **1a** and $Cu(OPiv)_2$ to produce the aza-heterocycle **2a** was conducted. The process was followed at temperatures between 60 and 80 °C and under equimolar concentration conditions of copper and imine ([Cu] = [**1a**] = 3.6×10^{-4} M). Even though experiments with [**1a**] = (2–5)×[Cu] were also conducted, neither qualitative nor quantitative differences were observed from the runs carried out under stoichiometric 1:1 conditions, indicating that the process monitored occurs after the complete coordination of **1a** to the Cu(II) center, producing the coordination complex **1aCu** (Scheme 2).[10] This approximation has already been found applicable for other labile species of Pd(II) and Rh(II).[4d–f,5b,c,18]

These **1a** + $Cu(OPiv)_2$ above mentioned experiments produced reproducible data, despite the fact that errors larger than the standard were obtained, which has to be attributed to the harsh reaction conditions used (60–80 °C during 30–100 h). Furthermore, the presence of metallic copper in the reaction medium (as evidenced PXRD after centrifugation of the final reaction mixtures) may produce an undesired shifting of the final absorbance, albeit as a minor effect. In all cases, the changes observed in the UV-Vis spectra for the process could only be fitted satisfactorily using a two-step process by the standard Specfit or ReactLab global analyses software (see Figure S1a–c in the Supporting Information).[14] Up to 3–5 replicates were conducted for each run with excellent agreement, wherefrom two first-order rate constants were derived. Figure 1a features the temperature-dependence of the average values obtained at each temperature according to the standard Eyring plots, providing the thermal activation parameters for the first-order reaction steps observed (Table 1). Even though the temperature range is not very large; 20 degrees is normally accepted as a reliable temperature amplitude whenever a good linearity in the Eyring plots is obtained (as seen in the Figures 1 and 2).[19] Furthermore, a 10 degree decrease in temperature would lead to extended reaction monitorings up to 1–2 weeks, which could be rather unreliable, while higher temperatures over the boiling point of the solvent (acetonitrile) are not advisable.

As the UV-Vis monitoring of the experiments allowed for fitted time-resolved concentration profiles (Figure 1b), batch experiments were conducted under similar conditions in order to elucidate the nature of the dominant species within this time-profile. Direct MS-ESI measurements of the reaction sample at 3 h shows the diagnostic m/z 270.1 peak (see Figure S2 in the Supporting Information), assigned to $\{((\mathbf{1a})Cu^{II}(CH_3CN)) + 1e^-\}^+$ which corresponds to the copper(II) coordination complex with **1a** where the pivalate ligand has been

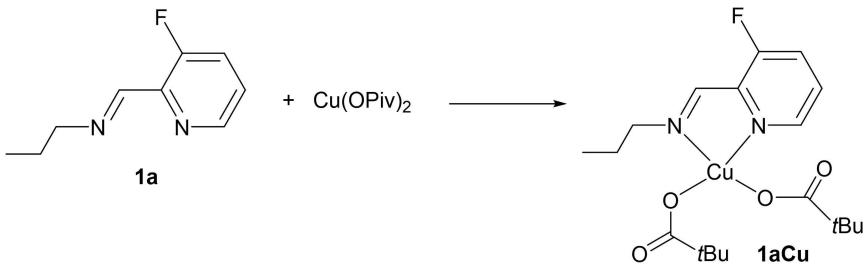

Scheme 2. Scheme featuring the formation of the coordination complex **1aCu**.[10]

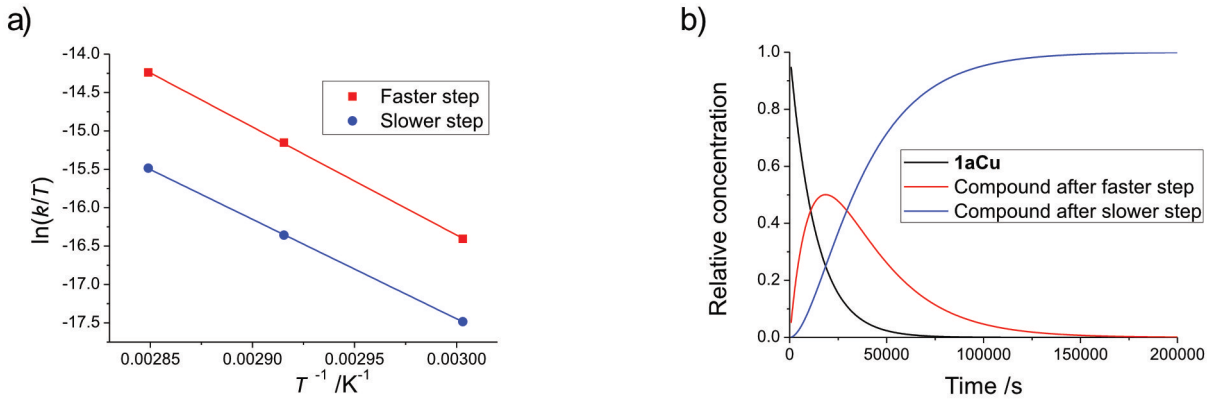

Figure 1. a) Eyring plots of the temperature dependence for the first-order rate constants of the two steps observed for the stoichiometric reaction of **1a** and $Cu(OPiv)_2$. b) Time-resolved concentration profiles for the two-step process observed on reaction mixtures of **1a** and $Cu(OPiv)_2$ at 3.6×10^{-4} M concentration at 70 °C in acetonitrile solution.

Research Article
doi.org/10.1002/ejic.202400564

Table 1. Kinetic (at 343 K) and thermal activation parameters derived from the temperature dependence for the first-order rate constants of the two-step process observed for the stoichiometric reaction of **1a** + $Cu(OPiv)_2$ and **1a** + $Cu(OPiv)_2$ + DDQ.

Reaction	Reaction	$^{343}k/s^{-1}$	$\Delta H^{\neq}$/kJ mol^{-1}	$\Delta S^{\neq}$/J K^{-1} mol^{-1}
1a + $Cu(OPiv)_2$	Faster step	9.0×10^{-5}	117 ± 1	17 ± 2
	Slower step	2.7×10^{-5}	108 ± 1	−20 ± 2
1a + $Cu(OPiv)_2$ + DDQ	Faster step	Equal to those for the 1a + $Cu(OPiv)_2$ reaction above		
	Slower step	7.2×10^{-6}	101 ± 5	−41 ± 1

exchanged by an acetonitrile solvent molecule. The detection of this species can be justified by a plausible reduction of the copper(II) species during analysis, in agreement with literature reports.[20] After 12 hours a new signal at m/z 268.0 appears and becomes dominant after 90 h of reaction monitoring; this signal is associated to a coordination copper complex with the imidazo[1,5-*a*]pyridine **2a**, $\{((\mathbf{2a})Cu^{I}(CH_3CN)) + 1e^{-}\}^{+}$. Interestingly, a m/z 269.0 peak appears after 45 h, which provides experimental evidence of the pivotal cyclometalated intermediate **CM-I** as $\{(\mathbf{1a\text{-}H})Cu^{II}(CH_3CN)\}^{+}$. Based on this data, the reaction sequence observed fits with that indicated in Scheme 3; the first and faster step corresponding to the cyclometalation process produces the intermediate **CM-I** from **1aCu**, followed by a slower step leading to **2a** by reductive elimination. All attempts to isolate this intermediate species proved unsuccessful, the fact that even in the most favorable conditions the **CM-I** intermediate is only at a 40% relative concentration level, both the initial **1a** and the final cyclic compounds remaining at the 30% level, explains this difficulty. This type of reactivity has also been recently reported in the literature for other Cu(II)-catalyzed systems.[21]

As none of the above experiments proved the prevalence of the {2+} oxidation state of the copper center throughout the process, batch experiments were conducted at 78 °C for 24 h to gain a better insight on the copper species involved by time-resolved electron spin resonance (ESR) spectroscopy. The spectra collected at 77 K (Figure S3a) show a rather complex mixture of Cu(II) species, probably due to the freezing of equilibrium mixtures of coordination compounds, while at 298 K the spectra proved to be much more indicative (probably due to the averaging of the equilibrium mixtures Figure S3b). Figure 2a features the stacked ESR spectra of a freshly prepared [Cu] = [**1a**] = 5×10^{-4} M sample in acetonitrile, and the reaction mixture after 45 min and 3 h at 78 °C. The similarity among the three spectra indicates the presence of Cu(II) species in all cases. This uniformity in the shape of the ESR spectra is maintained for

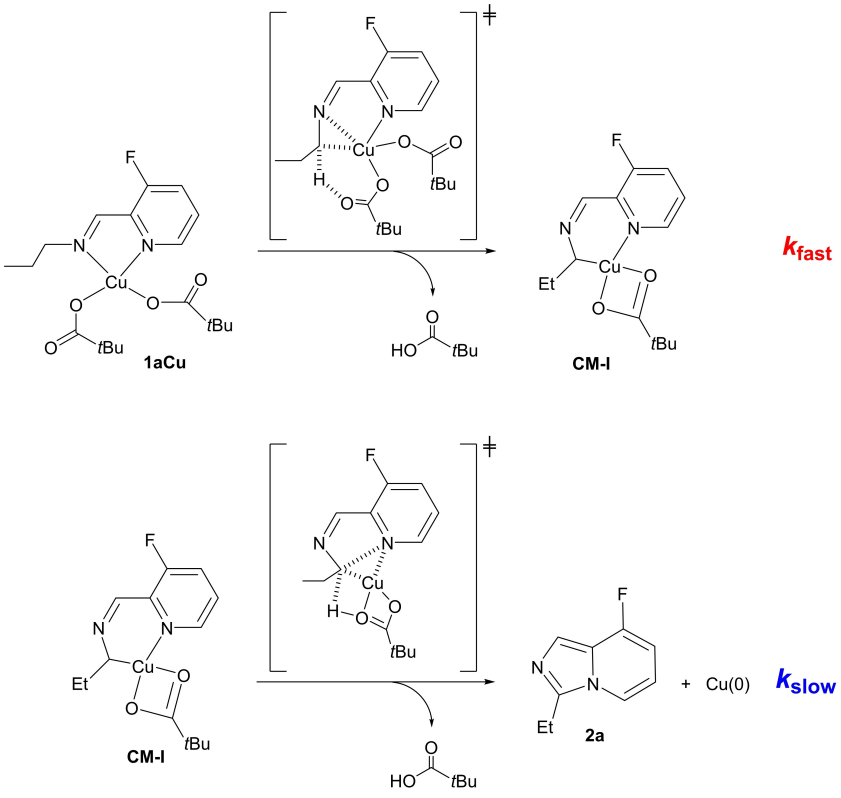

Scheme 3. Proposed reaction sequence for the formation of **2a** from the coordination complex **1aCu** (values of k_{fast} and k_{slow} are collected in Table 1).

Research Article
doi.org/10.1002/ejic.202400564

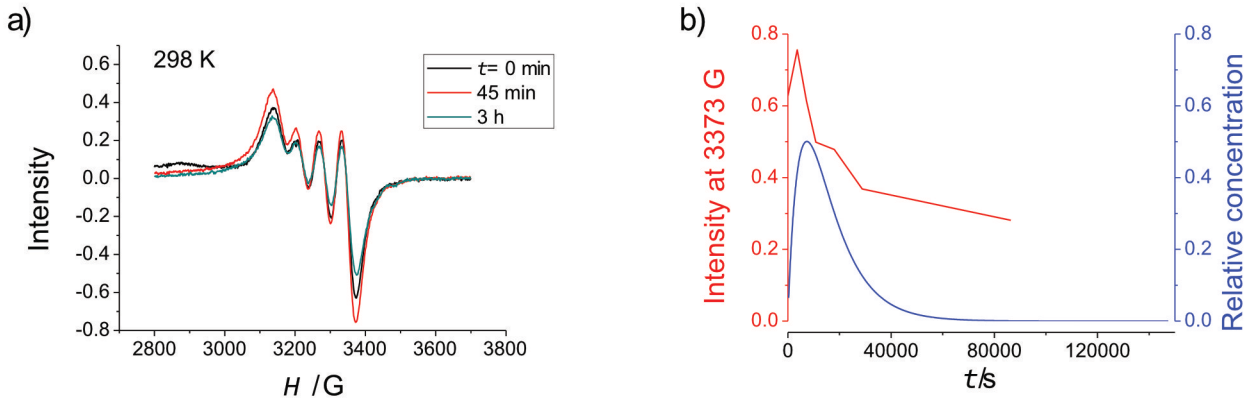

Figure 2. a) 298 K ESR spectra of a freshly prepared [Cu] = [**1a**] = 5×10^{-4} M sample in acetonitrile at room temperature (black); after 45 min (red) and after 3 h at 78 °C (blue). b) Time evolution of the intensity of the signal at 3373 G for the ESR spectra collected (red) and calculated concentration profile for compound **CM-I** (blue) from Table 1 data.

24 h; at longer times, the intensity of the signal decreases with a concomitant appearance of metallic copper in the reaction vessel (see above). Figure 2b collects the time-resolved intensity of the signal (measured at 3373 G) and the calculated concentration profile of **CM-I**, according to the rate constants indicated in Table 1. Despite the different experimental setups used for ESR and UV-Vis monitoring of the reaction, the time-profiles obtained are quite similar in both cases. The ESR spectral trends suggest that the initial **1aCu** complex evolves to the putative **CM-I** species, as evidenced by an increase in intensity of the signal arising from a Cu(II) center with axial symmetry and, after this initial increase, the intensity decreases as a result of metallic copper precipitation and the formation of **2a**.

The values derived for the thermal activation parameters indicated in Table 1 for the cyclometalation process (*i.e.* formation of **CM-I**, k_{fast}) agree with important enthalpy demands, even for these base-assisted proton abstractions, as expected for the activation of rather strong C(sp^3)–H bonds. The values of the activation entropies are small, indicating that the elongation of both the C–H bond and the copper coordination sphere offset the intuitive ordering on going to the transition state proposed in Scheme 3. The CMD reactivity shown seems the most adequate to explain the transition state of the reaction observed. Although this mechanism has been found operative in a wealth of similar and related systems involving heavy metals (such as Pd(II), Pt(II), Rh(I), Rh(II)),[5b,22] for lighter metals such as copper the amount of literature data is rather scarce.[23] As for the reductive elimination/proton abstraction slower step, k_{slow}, the enthalpy demands are again rather large, but the value of the activation entropy is definitively more negative than for the C(sp^3)–H bond activation, as would be expected from the higher ordered transition state indicated in Scheme 3, despite the Cu–N and Cu–C expected bond elongation.

2.1.2. Reaction in the Presence of DDQ

Aiming to the mechanistic understanding of the formation of **3a** in the Cu(II)-catalyzed process in the presence of DDQ (Scheme 1), we checked the reactivity of the isolated imidazo-pyridine **2a** with by DDQ. Interestingly, the isolated neat cooper-free compound **2a** *plus* DDQ did not produce **3a** neither in the presence nor absence of $Cu(OPiv)_2$. Alternatively, the final reaction mixture obtained after the full reaction sequence indicated in Scheme 3, was also treated further with stoichiometric and 5-fold excess of DDQ and monitored by time-resolved UV-Vis spectroscopy. A series of complex changes, ranging from seconds to hours at room temperature were observed, but time-resolved HPLC/HRMS monitoring of the reaction mixtures indicates again the absence of compound **3a**, even after 24 h of reaction at 70 °C.

Taking into account the initial control carried out using pure isolated **2a**, the reactivity observed by UV-Vis time-monitored changes should thus correspond to an independent reaction of DDQ with **2a**, copper pivalate being irrelevant for this stage. Effectively, the quantitative formation of a **2a-DDHQ** adduct was seen to occur on reaction of **2a** with DDQ in less than 30 minutes at room temperature (see Figure S4 in the Supporting Information). The process, involving a reactivity already described in the literature,[24] corresponds to a dead-end reaction of the catalytic process from **2a**, as isolated **2a-DDHQ** is also stable in the presence of $Cu(OPiv)_2$. Moreover, when the **2a-DDHQ** adduct was treated with imine **1b** and $Cu(OPiv)_2$ (1.5 equivalents) at 100 °C for 10 min under microwave irradiation neither **3a** nor **3b** products could be detected, ruling out both its role as reaction intermediate and cyanating agent.

Taking into account that compound **3a** is formed under catalytic conditions in the presence of DDQ (see Figure S5 in the Supporting Information), these results indicate that the addition of the cyanide group to the **1a** structure has to occur either on *i*) the **1a** imine, *ii*) the coordinated **1aCu** complex, or *iii*) the cyclometallated **CM-I** pivotal structure produced after the fast step of the reactivity observed (Scheme 3, Figure 1b). In

Research Article
doi.org/10.1002/ejic.202400564

this respect, neither a cyanated **1 a** imine nor a cyanated **1aCu** coordination species have been observed in the direct injection HRMS experiments of the reaction mixture, ruling out *i*) and *ii*) processes. Thus, cyanation should take place on the cyclometallated **CM-I** intermediate to produce the corresponding **CM-II** (reaction *iii*). This process has to be competing favorably, in kinetic terms, with the dead-end path leading to the **2 a-DDHQ** formation reaction (Scheme 4).

Once the reactivity involving the formation of the non-cyanated **2 a** compound was established kinetico-mechanistically, the investigation of the reaction of Cu(II) pivalate and **1 a** to produce the **3 a** cyanated-heterocycle was pursued *via* UV-Vis time-resolved monitoring. The process was followed on an equimolecular ternary (1 : 1 : 1) mixture of **1 a** + $Cu(OPiv)_2$ + DDQ in acetonitrile solution at the 3.6×10^{-4} M concentration scale.

The time-resolved UV-Vis spectral changes observed for these runs in the initial 30–100 min time-scale after mixing the reactants at 70 °C are extremely complex, although very reproducible (see Figure S6 in the Supporting Information). In all cases they are poorly-defined, indicating that (apart from possible DDQ secondary reactivity) they might correspond to a fast reaction occurring on some compound being formed at a later stage in the full process, thus becoming kinetically quasi-silent.[25] In any case, the ill definition of these fast UV-Vis spectral changes does not allow for any kinetic quantification, and the absence of these changes in the previously studied reaction of **1 a** + $Cu(OPiv)_2$ indicates that they effectively refer to reactions involving DDQ. Contrarily, at longer time-scales two very well-defined changes were observed, which exhibited spectral changes equivalent to those obtained for the reaction of **1 a** with $Cu(OPiv)_2$. Using the same procedures indicated before, these changes could be fitted to a set of two sequential

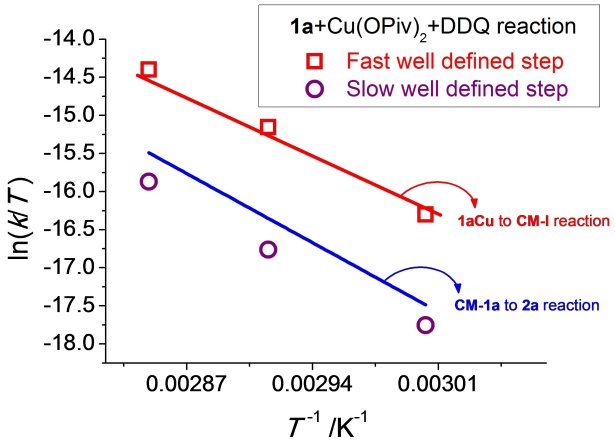

Figure 3. Eyring plots of the temperature dependence for the first-order rate constants of the two-steps observed for the stoichiometric reaction of **1 a** + $Cu(OPiv)_2$ + DDQ. Straight lines correspond to the thermal activation parameters indicated in Table 1 for the parent **1 a** + $Cu(OPiv)_2$ reaction.

first-order processes, producing very reproducible values (3–5 repeats) despite the errors involved. Figure 3 shows how the temperature dependence of these values relate with the data that have been associated to the formation of the intermediate cyclometalated **CM-I** (red line), and the final **2 a** species (blue line). The derived kinetic and thermal activation data derived from these Eyring plots are also collected in Table 1.

Clearly, the data collected indicates that the cyclometallation reaction of the coordination compound **1aCu** to form **CM-I**, even in the presence of DDQ, is still the faster step of the full process leading to **3 a** (Figure 3, red square data). As cyanation of **CM-I** to **CM-II** has been proved to be much faster than the

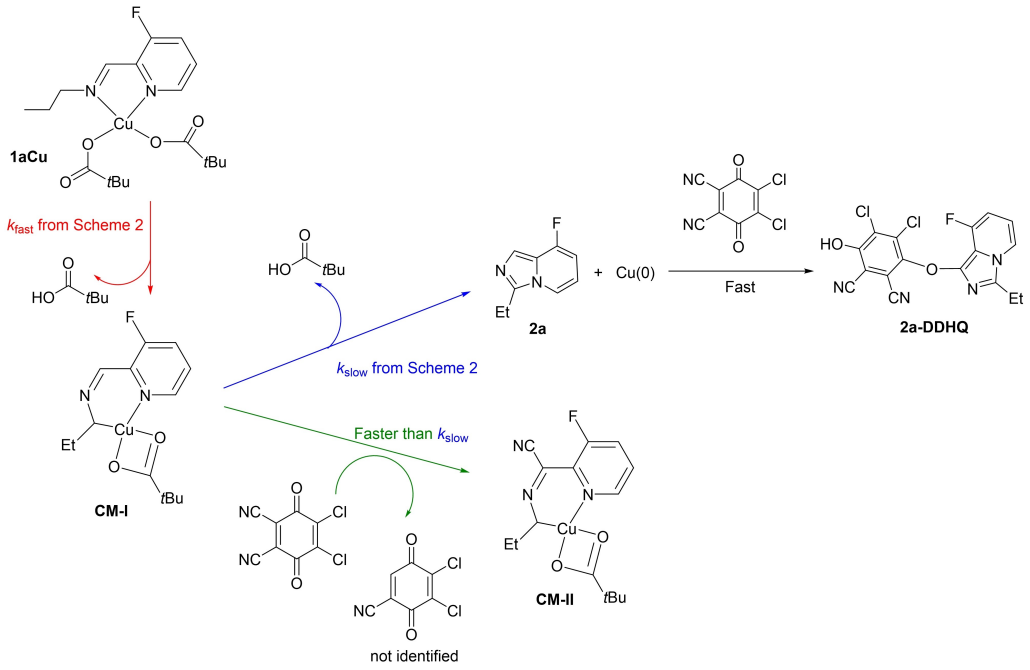

Scheme 4. Proposed reaction pathways from **CM-I** in the presence of DDQ.

Research Article
doi.org/10.1002/ejic.202400564

reductive elimination to produce **2 a** (Scheme 4), the ill-defined reactivity observed in the minute's timescale should correspond, at least in part, to this process. Furthermore, as the rate of cyanation of **CM-I** is necessarily at least first order with respect to DDQ, it is expected to be much faster under catalytic conditions (where [DDQ]⋙[Cu]) remaining unobserved under those preparative experimental conditions. The reductive elimination/proton abstraction to form **3 a** should then be the slower rate-determining step observed under those conditions (Figure 3, purple circle data).

In order to ascertain the nature of the time-resolved speciation of the compounds involved in the full reactivity, HPLC/(HR)MS (see Table S2 in the Supporting Information) was conducted at kinetically selected times from batch experiments at 70 °C. After 2 h the signal associated to compound **1 a** ({**1 a** + H^+} m/z 167.10) is not found any more in the reaction mixture, while the cyclometallated compound **CM-I** ({**CM-I** − $1e^-$} m/z = 329.07 appears in a steady-state concentration level for most of the reaction time (see Figure S7 in the Supporting Information). Interestingly, while no signals associated to **2 a** or **2 a-DDHQ** are observed (indicating that the process in Scheme 3, top, is not operating), the intensity of the signal attributed to **CM-I** decreases and a signal attributed to the cyanated **CM-II** structure ({**CM-II** + **MeCN** $-1e^-$} m/z = 395.11) increases its intensity during 24 h; after this time the intensity of this signal decreases (see Figure S8 in the Supporting Information). The detection of these species could be explained by electron ejection from the sample in the mass chamber, triggering either a Cu(II)-Cu(III) oxidation,[7–8,12] or by ligand one-electron oxidation.[13] In parallel, the signal associated to compound **3 a** appears as the final compound of the process.

As a whole, the reactivity observed both *via* time-resolved UV-Vis and HPLC/HRMS monitoring could be summarized as in Scheme 5. From the data of Table 1, it is also interesting to note that the reductive elimination/proton abstraction process from the cyanated **CM-II** derivative is, in fact, counter-intuitively slower than that from the parent non-cyanated **CM-I** analogue. Nevertheless, as the cyanation process is faster than the reductive elimination from the non-cyanated **CM-I**, and not rate determining, the formation of **3 a** without the presence of any **2 a** derivative is accomplished. The fact that the solely reason for this rate difference involves the activation entropy (Table 1) makes discussion rather difficult, as enthalpy would be expected to have a key role due the electron-withdrawing character of the CN group, which should increase the acidity of the Cu(II) center. An associated decrease in the Cu–C and Cu–O bond elongation in the transition state, for the cyanated system with respect to the parent non-cyanated analogue, due to the reason above could be held responsible for the distinct behavior.

3. Conclusions

The kinetico-mechanistic study of the stoichiometric processes occurring on the Cu(II) and carboxylate-assisted synthesis of imidazo[1,5-*a*]pyridines has enabled to propose a reaction sequence based on a CMD pathway; namely, the formation of Cu(II)-based intermediates has been experimentally evidenced by time-resolved ESR. The process involves a C–H bond activation followed by a reductive elimination/proton abstraction, both being high enthalpy demanding and with little entropy decrease, despite the high order transition state. The latter must be associated to bond elongation events in order to reach the proposed transition state. In the presence of a cyanating agent, the cyclometallated intermediate **CM-I** initially formed after the C–H bond activation undergoes C(sp^2)–H bond cyanation prompting the introduction of the cyano group, thus switching off the formation of the expected imidazo[1,5-*a*]pyridine **2 a**; instead, the more energy demanding formation of the cyano-based imidazo[1,5-*a*]pyridine **3 a** is attained.

Acknowledgements

We acknowledge Giuseppe Sciortino and Gregori Ujaque Pérez (Universitat Autònoma de Barcelona) for helpful discussions on the reaction mechanism. D.P. and M.G. thanks the Centre National de la Recherche Scientifique (CNRS) and the University Toulouse 3-Paul Sabatier for the financial support. The valuable help of Dr. Núria Clos in the ESR analyses is gratefully acknowledged.

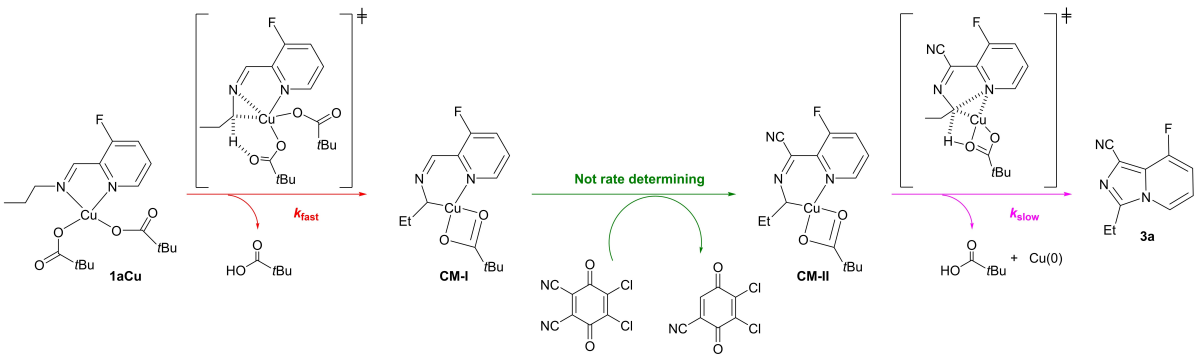

Scheme 5. Proposed mechanistic pathway for the formation of **3 a** in the presence of DDQ.

Conflict of Interests

The authors declare no conflict of interest.

Data Availability Statement

The data that support the findings of this study are available in the supplementary material of this article.

Keywords: Copper · Carbon-hydrogen bond activation · DDQ-mediated cyanation · kinetico-mechanistic studies

[1] a) J. Loup, U. Dhawa, F. Pesciaioli, J. Wencel-Delord, L. Ackermann, *Angew. Chem. Int. Ed.* **2019**, *58*, 12803–12818; b) B. Su, Z.-C. Cao, Z.-J. Shi, *Acc. Chem. Res.* **2015**, *48*, 886–896; c) P. Gandeepan, T. Müller, D. Zell, G. Cera, S. Warratz, L. Ackermann, *Chem. Rev.* **2019**, *119*, 2192–2452; d) D. Pla, M. Gomez, *ACS Catal.* **2016**, *6*, 3537–3552.

[2] a) G. Evano, N. Blanchard, M. Toumi, *Chem. Rev.* **2008**, *108*, 3054–3131; b) M. Camats, D. Pla, M. Gómez, *Nanoscale* **2021**, *13*, 18817–18838; c) Y. Yang, W. Gao, Y. Wang, X. Wang, F. Cao, T. Shi, Z. Wang, *ACS Catal.* **2021**, *11*, 967–984; d) M. L. Kantam, C. Gadipelly, G. Deshmukh, K. R. Reddy, S. Bhargava, *Chem. Rec.* **2019**, *19*, 1302–1318.

[3] a) G. Aullón, M. Crespo, M. Font-Bardia, J. Jover, M. Martínez, J. Pike, *Dalton Trans.* **2015**, *44*, 17968–19969; b) G. Aullón, M. Crespo, J. Jover, M. Martínez, in *Chapter Five – Diarylplatinum(II) Scaffolds for Kinetic and Mechanistic Studies on the Formation of Platinacycles via an Oxidative Addition/Reductive Elimination/Oxidative Addition Sequence*, Eds.: R. V. Eldik, C. Hubbard), Academic Press, **2017**, pp. 195–242;c) T. Calvet, M. Crespo, M. Font-Bardia, S. Jansat, M. Martínez, *Organometallics* **2012**, *31*, 4367–4373.

[4] a) K. M. Altus, J. A. Love, *Commun. Chem.* **2021**, *4*, 173; b) J. Calleja, D. Pla, T. W. Gorman, V. Domingo, B. Haffemayer, M. J. Gaunt, *Nat. Chem.* **2015**, *7*, 1009–1016; c) R. T. Gephart III, T. H. Warren, *Organometallics* **2012**, *31*, 7728–7752; d) E. Laga, A. García-Montero, F. J. Sayago, T. Soler, S. Moncho, C. Cativiela, M. Martínez, E. P. Urriolabeitia, *Chem. Eur. J.* **2013**, *19*, 17398–17412; e) S. Garcia-Granda, P. Lahuerta, J. Latorre, M. Martínez, E. Peris, M. Sanau, M. Ubeda, *J. Chem. Soc., Dalton Trans.* **1994**, 539–544; f) G. González, P. Lahuerta, M. Martínez, E. Peris, M. Sanaú, *J. Chem. Soc., Dalton Trans.* **1994**, 545–550.

[5] a) S. I. Gorelsky, D. Lapointe, K. Fagnou, *J. Am. Chem. Soc.* **2008**, *130*, 10848–10849; b) G. Aullón, R. Chat, I. Favier, M. Font-Bardia, M. Gómez, J. Granell, M. Martínez, X. Solans, *Dalton Trans.* **2009**, 8292–8300; c) M. Gómez, J. Granell, M. Martínez, *Organometallics* **1997**, *16*, 2539–2546.

[6] Y. Boutadla, D. L. Davies, S. A. Macgregor, A. I. Poblador-Bahamonde, *Dalton Trans.* **2009**, 5820–5831.

[7] a) W. Zhang, F. Wang, S. D. McCann, D. Wang, P. Chen, S. S. Stahl, G. Liu, *Science* **2016**, *353*, 1014–1018; b) J. K. Bower, M. S. Reese, I. M. Mazin, L. M. Zarnitsa, A. D. Cypcar, C. E. Moore, A. Y. Sokolov, S. Zhang, *Chem. Sci.* **2023**, *14*, 1301–1307.

[8] a) X. Wu, Y. Zhao, G. Zhang, H. Ge, *Angew. Chem. Int. Ed.* **2014**, *53*, 3706–3710; b) S. D. McCann, S. S. Stahl, *Acc. Chem. Res.* **2015**, *48*, 1756–1766; c) B. L. Tran, B. Li, M. Driess, J. F. Hartwig, *J. Am. Chem. Soc.* **2014**, *136*, 2555–2563.

[9] a) G. K. Reen, A. Kumar, P. Sharma, *Beilstein J. Org. Chem.* **2019**, *15*, 1612–1704; b) J. Tang, B. Wang, T. Wu, J. Wan, Z. Tu, M. Njire, B. Wan, S. G. Franzblauc, T. Zhang, X. Lu, K. Ding, *ACS Med. Chem. Lett.* **2015**, *6*, 814–818; c) R. R. Knapp, V. Tona, T. Okada, R. Sarpong, N. K. Garg, *Org. Lett.* **2020**, *22*, 8430–8435.

[10] M. Camats, I. Favier, S. Mallet-Ladeira, D. Pla, M. Gómez, *Org. Biomol. Chem.* **2022**, *20*, 219–227.

[11] a) M. A. Gonzálvez, C. Su, C. M. Williams, P. V. Bernhardt, *Chem. Sci.* **2022**, *13*, 10506–10511; b) M. A. Gonzálvez, C. M. Williams, M. Martínez, P. V. Bernhardt, *Inorg. Chem.* **2023**, *62*, 4662–4671.

[12] W. Yan, A. T. Poore, L. Yin, S. Carter, Y.-S. Ho, C. Wang, S. C. Yachuw, Y.-H. Cheng, J. A. Krause, M.-J. Cheng, S. Zhang, S. Tian, W. Liu, *J. Am. Chem. Soc.* **2024**, *146*, 15176–15185.

[13] I. M. DiMucci, J. T. Lukens, S. Chatterjee, K. M. Carsch, C. J. Titus, S. J. Lee, D. Nordlund, T. A. Betley, S. N. MacMillan, K. M. Lancaster, *J. Am. Chem. Soc.* **2019**, *141*, 18508–18520.

[14] a) M. Maeder, P. King, in *ReactLab*, Vol. Jplus Consulting Pty Ltd, East Fremantle, WA. Australia, **2009**; b) R. A. Binstead, A. D. Zuberbuhler, B. Jung, in *SPECFIT32*, Vol. Spectrum Software Associates, Marlborough, MA, USA, **2005**.

[15] a) A. de Juan, M. Maeder, M. Martínez, R. Tauler, *Chemom. Intell. Lab. Syst.* **2000**, *54*, 123–141; b) A. de Juan, M. Maeder, M. Martínez, R. Tauler, *Anal. Chim. Acta* **2001**, *442*, 337–350.

[16] J. Serrano-Plana, W. N. Oloo, L. Acosta-Rueda, K. K. Meier, B. Verdejo, E. García-España, M. G. Basallote, E. Münck, L. Que, Jr., A. Company, M. Costas, *J. Am. Chem. Soc.* **2015**, *137*, 15833–15842.

[17] a) T. Calvet, M. Crespo, M. Font-Bardia, K. Gómez, G. González, M. Martínez, *Organometallics* **2009**, *28*, 5096–5106; b) G. Aullón, S. Jansat, K. Gómez, G. González, M. Martínez, R. Poli, M. Rodriguez-Zubiri, *Inorg. Chem.* **2011**, *50*, 5628–5636.

[18] D. Aguilar, R. Bielsa, M. Contel, A. Lledós, R. Navarro, T. Soler, E. P. Urriolabeitia, *Organometallics* **2008**, *27*, 2929–2936.

[19] a) M. A. Gonzálvez, P. V. Bernhardt, M. Font-Bardia, A. Gallen, J. Jover, M. Ferrer, M. Martínez, *Inorg. Chem.* **2021**, *60*, 18407–18422; b) L. Alcázar, P. V. Bernhardt, M. Ferrer, M. Font-Bardia, A. Gallen, J. Jover, M. Martínez, J. Peters, T. J. Zerk, *Inorg. Chem.* **2018**, *57*, 8465–8475.

[20] H. Lavanant, H. Virelizier, Y. Hoppilliard, *J. Am. Soc. Mass Spectrom.* **1998**, *9*, 1217–1221.

[21] I. M. Blythe, J. Xu, J. S. Fernandez Odell, J. W. Kampf, M. A. Bowring, M. S. Sanford, *J. Am. Chem. Soc.* **2023**, *145*, 18253–18259.

[22] a) P. E. Piszel, B. J. Orzolek, A. K. Olszewski, M. E. Rotella, A. M. Spiewak, M. C. Kozlowski, D. J. Weix, *J. Am. Chem. Soc.* **2023**, *145*, 8517–8528; b) Y. Boutadla, D. L. Davies, S. A. Macgregor, A. I. Poblador-Bahamonde, *Dalton Trans.* **2009**, 5820–5831; c) E. Clot, O. Eisenstein, N. Jasim, S. A. Macgregor, J. E. McGrady, R. N. Perutz, *Acc. Chem. Res.* **2011**, *44*, 333–348; d) R. N. Perutz, S. Sabo-Etienne, A. S. Weller, *Angew. Chem. Int. Ed.* **2022**, *61*, e202111462; e) R. N. Perutz, S. Sabo-Etienne, *Angew. Chem. Int. Ed.* **2007**, *46*, 2578–2592; f) J. Granell, M. Martínez, *Dalton Trans.* **2012**, *41*, 11243–11258.

[23] a) S. Tang, T. Gong, Y. Fu, *Sci. China Chem.* **2013**, *56*, 619–632; b) G.-Y. Ruan, Y. Zhang, Z.-H. Qi, D.-X. Ai, W. Liu, Y. Wang, *Comput. Theor. Chem.* **2015**, *1054*, 16–21.

[24] a) V. S. Batista, R. H. Crabtree, S. J. Konezny, O. R. Luca, J. M. Praetorius, *New J. Chem.* **2012**, *36*, 1141–1144; b) A. S. Jalilov, J. Lu, J. K. Kochi, *J. Phys. Org. Chem.* **2016**, *29*, 35–41.

[25] a) J. H. Espenson, *Chemical Kinetics and Reaction Mechanisms*, McGraw-Hill, New York, **1981**; b) R. G. Wilkins, *Kinetics and Mechanisms of Reactions of Transition Metal Complexes*, VCH, Weinheim/New York, **1991**.

Manuscript received: August 30, 2024
Revised manuscript received: October 14, 2024
Accepted manuscript online: October 15, 2024
Version of record online: ■■, ■■

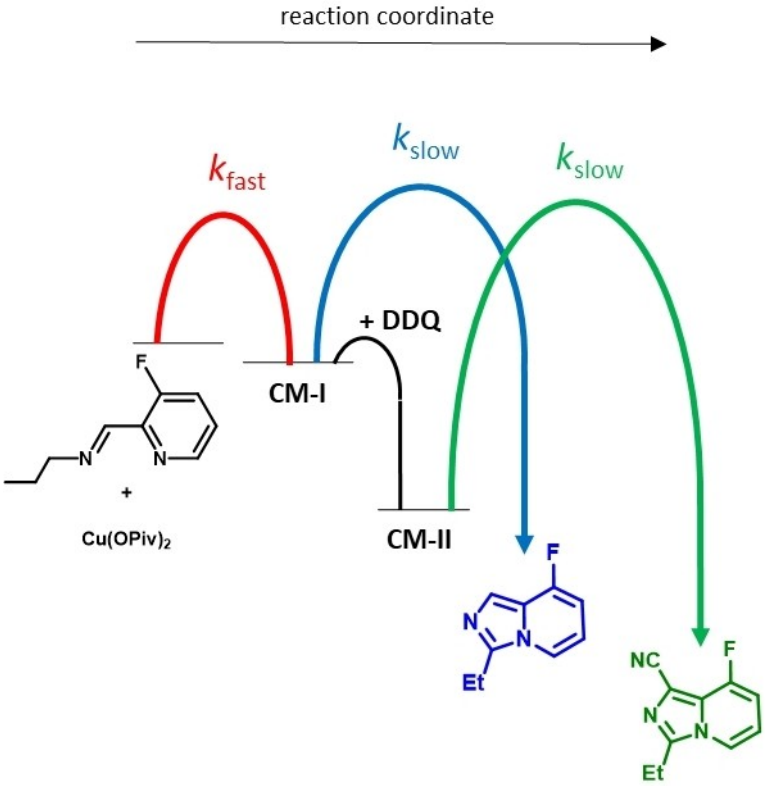

D. Pla, M. Ferrer, M. Gómez, M. Martinez Lopez**

The involvement of organometallic copper complexes in the synthesis of imidazo[1,5-*a*]pyridines from imines *via* sequential C–H bond activation processes has been evidenced by kinetico-mechanistic studies using operando UV-Vis reaction monitoring coupled to *ex-situ* analyses.